Investigation of the Neutral Gas Distribution on W7-AS Using the Monte-Carlo Code EIRENE in Combination with the Li-Beam Diagnostic

S. Fiedler, O. P. Heinrich, J. Das, K. McCormick and the W7-AS-Team
Max-Planck-Institut für Plasmaphysik, EURATOM Association,
D-85748 Garching, Germany

1. Introduction

The Li beam diagnostic on W7-AS /1/ allows the measurement of neutral density n_0 outside the plasma column as well as electron density profiles of the main plasma by observation of the collisionally induced LiI line radiation (671nm) from an injected high energy neutral Li-beam (20-66keV/0.5-3.0mA). Central profiles for higher densities are achieved by incorporating line integrated data from the HCN interferometer /2/. Thus highly accurate density profiles from the plasma middle to the walls are available. Using n_e-profiles and n_0 derived from the Li-beam in combination with H_α intensities measured at several points around the vessel, the Monte-Carlo code EIRENE is implemented to determine the important neutral sources as well as the absolute neutral density distribution.

2. Density profile reconstruction

For peak densities $n_{e0} < 4 \cdot 10^{19}$ m^{-3} profiles spanning the entire outer radius can be reconstructed by the Li beam diagnostic. Central profiles for higher densities are achieved, under the assumption of flat profiles, by incorporating data from HCN interferometry.

The HCN interferometer on W7-AS measures line densities along three parallel lines of sight in the φ=29° plane (approximate elliptical plasma cross section, cf. fig. 2.1). At low densities these data can be used to cross check the Li beam data. To this end the reconstructed Li density profiles are mapped along the magnetic surfaces using the TRANS-database to the plane of the HCN interferometer, integrated along the line of sights, and directly compared. Using the electron temperature profile as measured by Thomson scattering in the Li beam density reconstruction algorithm /3/ and a central beta consistent with the derived profile for the field line mapping, excellent agreement is found, cf. fig. 2.2. For higher central densities $n_0 \leq 1 \cdot 10^{20}$ m^{-3} the entire gradient region is still accessible by the Li beam diagnostic. The effective plateau value of the density profile can be calculated by subtracting the contribution of the plasma edge from the central HCN channel. A cubic spline approximation is used to construct a smooth transition between the edge density profile and the derived plateau value. To take into account possible uncertainties in the Li beam density profile, the plateau value is varied in such a way that the line integral of the smoothed density profile fits the line density of the HCN interferometer to within a tolerance of less then 2%. The outermost channel of the HCN interferometry is used to check the field line mapping. For the EIRENE calculation below a low iota (ι_a=0.34, no islands at the plasma edge), medium density (small beta effects) shot (#33359) is chosen. The derived density profile for this shot together with the edge density profile measured by the Li beam diagnostic is shown in fig. 2.3. Measurements of this quality can be routinely carried out on a ms time scale.

3. Neutral density measurements

The neutral density is registered in the injection port by observing the Li_{2p} line radiation from the Li beam induced by collisions between Li beam atoms and neutral particles. The observation volume is at a point 0.55 m from the plasma surface, thereby minimizing any interference from background light at the Li(2p) wavelength while maintaining a good vacuum conductance to the main vessel. The signal is calibrated by injection of the Li beam into the discharge chamber at known molecular gas pressure and applied magnetic field. Since EIRENE calculations indicate that molecules make up 99% of the neutral density within the injection port, this calibration may be directly applied to measurements performed during plasma discharges. For the discharge under investigation, see the EIRENE calculation below, the neutral density is determined to be $n_0 = 3.6 \cdot 10^{17}$m^{-3} ($1.5 \cdot 10^{-5}$ mbar).

4. H_α measurements

H_α intensities are recorded at different toroidal positions (cf. fig. 5.5): (1) spatially resolved by a diode array at the inner limiter, (2) at $\varphi=10°$, (3) at $\varphi=18°$, the position of the Li beam diagnostic and (4) at $\varphi=23°$. Data for positions 2-4 are absolutely calibrated via an Ulrich sphere (e.g. $H_\alpha(\varphi=18°) = 1.8 \cdot 10^{18}$ photons $m^{-2}s^{-1}sr^{-1}$) and used in the EIRENE calculations.

5. EIRENE simulation of H_α and n_o measurements

The neutral gas distribution plays a crucial role for source terms entering into the particle balance of the plasma edge and hence is an important component of edge investigations. To determine the absolute neutral density in the module of the Li beam, the neutral density distribution is calculated with the 3D Monte-Carlo code EIRENE /4/, using $n_e(r)$ profiles and n_o from the Li beam as well as the H_α intensity measured at 4 positions including the Li beam port and the poloidal H_α distribution at an inboard limiter. With these independently measured quantities n_o and H_α a consistency check of the EIRENE modelling of the neutral source locations is also possible. To properly accommodate the n_o measurement located deep inside a port, the Li beam port is also simulated as shown on the computational grid in fig. 5.1. Periodicity is assumed in the toroidal direction, i.e. each of the 5 modules is treated identically.

For clear conditions concerning neutral sources a discharge without islands (i_a=0.34) is considered, where the plasma has been shifted towards the inboard limiters (B_z=18mT) so that they comprise the main neutral source. The neutral source distribution is taken to be the same as the H_α intensity profile measured along the plasma-facing side of an inboard limiter.

This assumption yields self-consistent results: in fig. 5.3 the comparison between experimental and calculated H_α profiles shows good agreement over the entire limiter. Fig. 5.4 illustrates the corresponding lower inboard limiter and H_α line of sights, together with the neutral atom distribution. Since the distance of the Li beam to the inboard limiter is about 0.5 m toroidally and 150° poloidally, it is not clear a priori, which source dominates the local neutral density, i.e. the limiters or the global plasma-wall interaction. The scaling of the neutral particle distribution from the limiter source to its absolute H_α intensity shows that at the Li beam plane this source strength is too low for the corresponding H_α signal. This becomes clear from the toroidal variation of the neutral density shown in fig. 5.5: Between the limiter and Li beam plane the atomic density decays by 2 decades. Therefore a second source at the wall is introduced, which for simplicity is assumed to be a point source in the Li beam plane. It turns out that one has to put its location at the upper part of the so-called helical edge (corresponding to the upper tip of the plasma in fig. 5.1), which is expected to be the principal plasma-wall interaction area away from limiters. By scaling the point source neutral distribution with the H_α signal at the Li beam, n_o in the Li beam port and the next further H_α are predicted by the calculation to within 50%, whereas with other source locations the differences are more than an order of magnitude, if a reasonable solution exists at all. This shows that the helical edge defines the dominant region for the global plasma-wall interaction. In fig. 5.2 the toroidally and poloidally averaged atomic densities of the two sources are compared: inside the limiter the limiter source dominates the neutral density by a factor of 10, but outside the wall source is even higher than the latter.

6. Conclusions

Employing the Li beam $n_e(r)$ profiles and H_α intensities it has been possible to find a self-consistent 3D neutral source distribution in EIRENE showing that on the limiter the source profile corresponds roughly to the H_α intensity profile and that the helical edge is mainly responsible for the global plasma-wall interaction. In addition the neutral density in the Li beam port could be modelled for the first time, giving agreement within 50% to the experimental n_o value from the Li beam.

References:

/1/ K. McCormick, 21st EPS International Conference on Plasma Physics, Europhysics Conference Abstracts Vol. **18B**, Part III (1994) 1268

/2/ S. Fiedler, IPP-Report III/209 (October 1995)

/3/ J. Schweinzer, et al., Plasma Physics and Controlled Fusion, 34 (1992) 1173

/4/ D. Reiter, report of KFA-Jülich, Institut für Plasmaphysik, Nr. 2599 (1992)

2.1

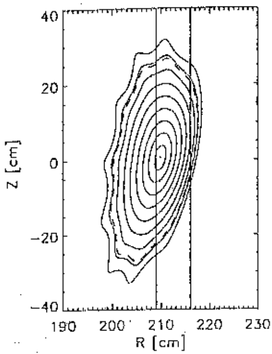

2.2

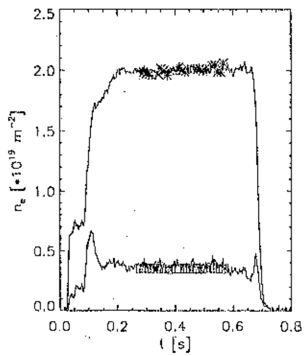

2.3

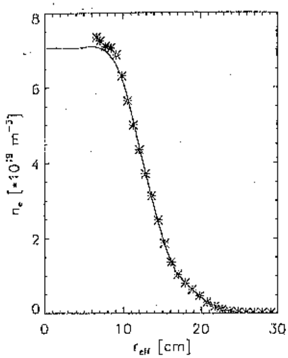

Fig. 2.1 Magnetic flux surfaces for discharge #34540 with line of sights for the HCN interferometer.

Fig. 2.2 Line densities of the HCN channels indicated in fig. 2.1 (solid lines) compared to the line integrals calculated from the Li beam data (symbols) for discharge #34540.

Fig. 2.3 Reconstructed profile using Li-beam edge density profile (symbols) and the central HCN chord for discharge #33359.

Fig. 5.1 Computational grid and diagnostics at the Li beam phi plane. The Li-beam n_e profile along the beam line is directly mapped onto the grid flux surfaces. Toroidally the grid has a resolution of 50 cells per module.

Fig. 5.2 Globally averaged atom density profile of the inboard limiter and the helical edge wall source with the Li beam n_e and Thomson temperature profile. The shadow line indicates the limiter position.

Fig. 5.3 Experimental and calculated H_α profiles at the lower inboard limiter. The tile index varies from bottom to top.

Fig. 5.4 Atomic density at the lower inboard limiter. The H_α intensity profile is used as the neutral source distribution.

Fig. 5.5 Toroidal atom density distribution of the limiter source on the flux surface in front of the inboard limiter for the half of one module. Higher values correspond to brighter colours. The upper picture shows along the poloidally averaged atomic density the toroidal positions of the inboard limiter (1), the Li beam plane (3) and two other H_α locations (2,4).

f005

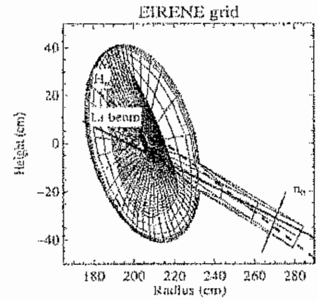

5.1

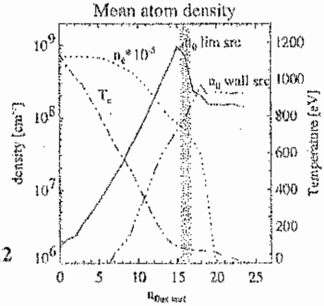

5.2

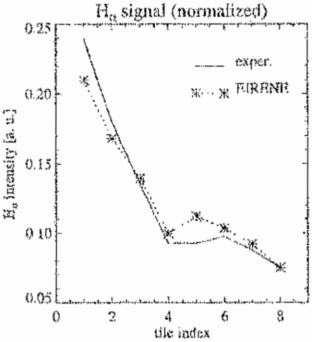

5.3

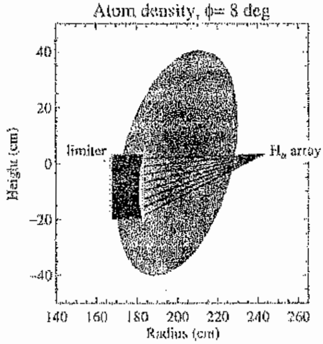

5.4

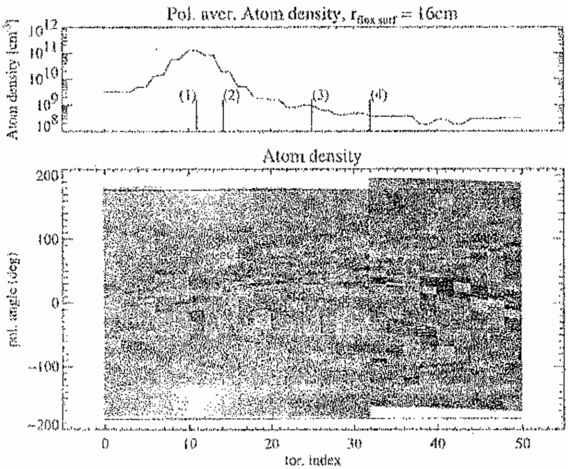

5.5